Anal Bioanal Chem (2012) 402:349–356
DOI 10.1007/s00216-011-5320-9

ORIGINAL PAPER

Label-free quantification of cystatin C as an improved marker for renal failure

Oliver Bleher · Markus Ehni · Günter Gauglitz

Received: 7 July 2011 / Revised: 29 July 2011 / Accepted: 4 August 2011 / Published online: 20 August 2011

Abstract A label-free biosensor has been developed, allowing quantification of cystatin C in human serum. This was achieved by using reflectometric interference spectroscopy as detection method. Cystatin C is a small serum protein that allows detection of renal failure more reliably than established parameters as creatinine. The protein was immobilized on the surface of a glass transducer, forming the sensitive layer of the sensor chip. Based on a binding-inhibition assay, two different types of monoclonal cystatin C antibodies were compared, by their behavior and their obtained working range in buffer and serum as matrix. Both antibodies allowed quantification of the protein in serum as matrix within the required clinical ranges of 0.53–1.02 mg/L. Detected recovery rates are in a range between 84.8% and 116.1%. The developed sensor shows high inner chip reproducibility and low cross-sensitivity.

Keywords Reflectometric interference spectroscopy (RIfS) · Optical sensors · Label-free detection · Renal failure · Cystatin C · Biosensor

Introduction

Renal function is determined by measuring the glomerular filtration rate (GFR), which is defined as the volume of fluid that is filtered by the kidney per unit of time. In routine clinical diagnostic, the GFR is evaluated by determination of the serum creatinine level. This method has been well established for decades [1], although there are some disadvantages. The serum creatinine level depends on various parameters, such as muscle mass, nutrition, gender, and age of the patient. Apart from that, the serum creatinine level will increase in case of a renal failure with a significant delay (so called "creatinine-blind range") which impedes early diagnostic and treatment [2, 3].

Therefore, alternative markers are needed that provide the possibility of identifying renal failure in an early stadium. Ideally, these markers are independent of other external influences such as nutrition and muscle mass.

The protein cystatin C is produced at a constant rate by almost all nucleated cell types and is eliminated from serum by glomerular filtration. The result is a constant serum level of cystatin C. Since numerous clinical studies showed that glomerular filtration is the only pathway to eliminate cystatin C from serum, it offers itself as a diagnostic marker for renal dysfunction [4, 5].

As a low-molecular mass protein, cystatin C is nearly completely reabsorbed and degraded through proximal tubular cells after filtration through the glomerular membrane. Urine concentration of cystatin C is therefore low in healthy individuals. In addition to its use as a GFR marker, cystatin C provides the opportunity for early detection of proximal tubular cell damage [6], which will cause a rise in urine cystatin C level.

Only two different reference ranges of cystatin C need to be differentiated in serum. For healthy individuals under 50 years of age, the normal range is in between 0.53 and 0.92 mg/L cystatin C. For individuals over 50 years of age, 0.58–1.02 mg/L is the normal range [7].

Today, cystatin C concentration can be determined by commercially available kits, which are mainly based on

Published in the *10th Anniversary Issue*.

O. Bleher (✉) · M. Ehni · G. Gauglitz
Institute of Physical and Theoretical Chemistry (IPTC),
Eberhard Karls University Tuebingen,
Auf der Morgenstelle 18,
72076 Tuebingen, Germany
e-mail: oliver.bleher@uni-tuebingen.de

enzyme methods. For routine use in central laboratories, these kits are too expensive.

Clinical routine diagnostic needs a fast, simple to use, and cheap detection method to establish cystatin C as an alternative marker for renal failure. Optical biosensors based on immunoassay principles can fulfill these requirements. These principles can be a direct assay, sandwich assay, or binding-inhibition assay [8, 9]. A direct assay is simple to perform, but it needs the antibody immobilized to the transducers surface, which can be a critical step and immobilized antibodies are not as stable as immobilized proteins. By trying to keep the assay as simple and stable as possible, we chose the binding-inhibition assay as the format. Here, only one type of antibody is needed and measurements can be kept simple and comparatively fast.

For detection, label-free optical techniques such as reflectometric interference spectroscopy (RIfS) [10], surface plasmon resonance (SPR) [11], or integrated optical devices [12] are of increasing relevance in the field of biosensors, as they leave the system of antigen and antibody unaffected by fluorescence- or radioactivity labels [13, 14].

RIfS is based on the reflection of white light at thin layers. White light from a halogen light source is guided to a transparent transducer consisting of multiple layers with thicknesses on a nanometer scale. The light is reflected at each interface, and the reflected beams interfere and result in characteristic interference spectra. Changes in the optical thickness of the sensitive layer cause a shift in the interference spectra. The optical thickness is defined as the product of the refractive index and the physical thickness of the layer. The optical thickness of the sensitive layer changes, e.g., when a receptor binds to a ligand immobilized to the surface. For this reason, binding events can be detected time resolved and nearly temperature independent during the measurement [15].

As this setup can be kept simple and provides the opportunity for miniaturization, it is possible to develop a portable device for point-of-care testing (POCT), which is a growing sector in medical diagnostics [16].

Based on RIfS, we established a label-free system based on antigen–antibody interaction that allows us to quantify cystatin C in human serum, within the relevant clinical ranges.

Materials and methods

Materials

RIfS transducer chips of 1 mm D263-glass substrate with a layer of 10 nm Ta_2O_5 and 330 nm SiO_2 on top are purchased from Schott AG, Mainz, Germany.

Common organic compounds are obtained from Fluka, Neu-Ulm, Germany; Sigma-Aldrich, Deisenhofen, Germany and Merck, Darmstadt, Germany.

3-Glycidyloxypropyl-trimethoxysilane (GOPTS) is purchased from Fluka Neu-Ulm, Germany.

Amino-functionalized dextran (AMD; 50% aminofunctions) is purchased from Innovent e.V. Jena, Germany.

Cystatin C is purchased from Scipak, Sittingbourne, UK.

Monoclonal mouse anti-cystatin C antibodies “Cyst28” (A) and “Cyst13” (B) are obtained from HyTest, Turku, Finland.

Human cystatin C-free serum is also purchased from HyTest, Turku, Finland.

Surface chemistry

Cleaning and activation of the surface

The transducer surface was cleaned and activated by ultrasonication with a freshly prepared solution of 60 vol. % concentrated H_2SO_4 and 40 vol.% H_2O_2 for 15 min. After that, the transducers are rinsed with Milli-Q water and dried in a nitrogen stream.

Silanization

Fifteen microliters of GOPTS is pipetted on the activated transducer. A second transducer is used to cover the first slide (“Sandwich”). After reacting for 1 h, the slides are rinsed with dry acetone and dried in a nitrogen stream.

Immobilization of the biopolymer

Ten microliters of AMD solution of 1 mg/μL in pure H_2O is pipetted on a silanized transducer. As in the previous step, a second slide is used to cover the first. After reaction for at least 12 h, the slides are thoroughly rinsed with Milli-Q H_2O and dried in a nitrogen stream.

Transformation of amino- to carboxyfunctions

To transform the amino- into carboxyfunctions, a solution of 2 mg/μL glutaric anhydrite (GA) in *N*,*N*′-dimethylformamide (DMF) is applied to the biopolymer surface of the transducer and covered with a second slide as in the previous step. After reaction for at least 12 h, the slides are rinsed with DMF and Milli-Q H_2O and dried in nitrogen stream.

Activation

To activate the surface carboxyfunctions a solution containing 1 M *N*-hydroxysuccinimide and 1.5 M diisopropyl-

carbodiimide in DMF is applied to the surface. Again, a second slide is used to form a "sandwich". After 4 h of reaction in a DMF atmosphere, the surface is rinsed with DMF and dry acetone and then dried in a nitrogen stream.

Immobilization of cystatin C

To the dried and activated surface, 7 μL of a solution containing 1 mg/mL cystatin C in phosphate-buffered saline (PBS) is pipetted. A second slide is used to form a "sandwich". After reaction for at least 12 h in a H_2O atmosphere, the transducers are rinsed with Milli-Q and stored under PBS at 4–8 °C.

Antigen/antibody treatment and storage

The antibodies are dissolved in PBS at pH 7.4 yielding to a stock solution of 1 mg/mL. The stock solution is stored in aliquots of 50 μL at −20 °C. Cystatin C is also dissolved in PBS yielding to a stock solution of 1 mg/mL. Aliquots of 50 μL are stored at −20 °C.

Binding-inhibition assay

A constant concentration of 1.5 mg/L cystatin C antibody is incubated with the sample, respectively defined concentrations of cystatin C, for 20 min at room temperature. The incubated sample is injected into the flow cell. The flow cell contains the sensor chip with its surface processed as described above. Antibodies binding to the immobilized cystatin C are detected via RIfS. Resulting binding signals are inversely proportional to the antigen concentration in the sample. The following Fig. 1 illustrates the procedure.

RIfS setup and data evaluation

The details of the setup have been described in previous publications [17, 18]. A Y-optical fiber guides the light from a halogen light source to the transducer. The white light is reflected at each interface of the transducer and the sensitive layer. The reflected beams are superimposed and are guided to a diode array spectrometer (Spekol 1100, Analytik Jena, Germany) forming an interference spectra. Binding events at the sensitive layer will cause a change in the optical thickness (refractive index multiplied by physical thickness) of this layer and therefore a shift in the interference spectra. This shift can be converted into a binding curve using internal software plotting optical thickness in nanometers versus time in seconds.

Fluid handling consists of an ASIA flow injection analysis by Ismatec, Germany with two independent pumps, a load/inject- and a six-way valve.

The different steps of a measurement cycle can be divided into a baseline, followed by the injection of 1 mg/mL ovalbumin, respective fetal-calf-serum (FCS) for serum measurements, to block unspecific binding. After blocking, the incubated sample is injected. Subsequently, the sensitive layer is regenerated with sodium dodecyl sulfate (SDS; 0.5%, pH 2).

Calibration

To calibrate the different antibody types in buffer and serum as matrix, every cystatin C concentration was determined threefold. During the first run, every concentration is determined once beginning with the

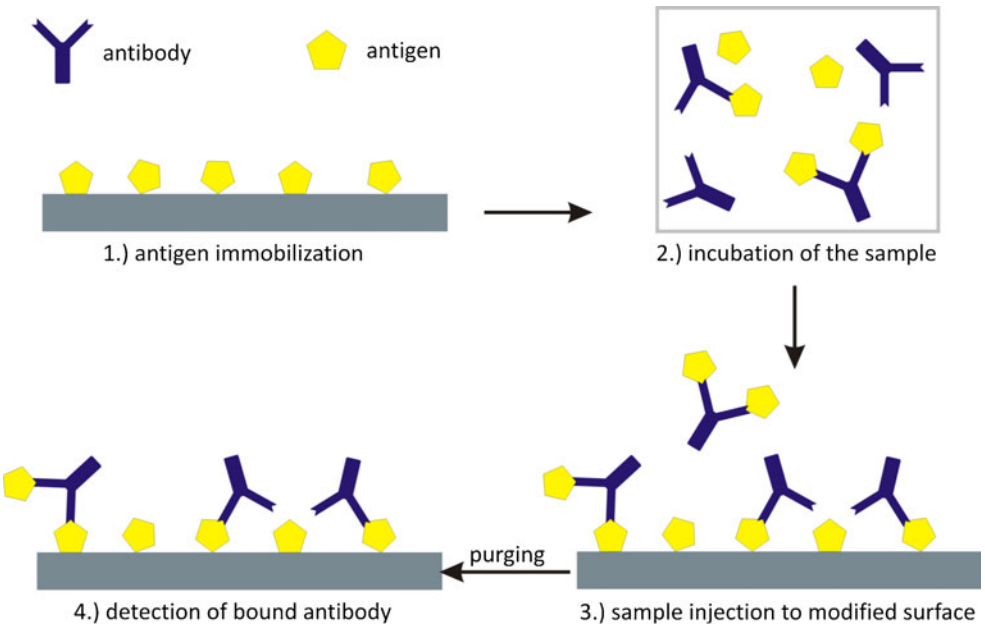

Fig. 1 Procedure of a binding-inhibition assay. In the first step, the antigen (*yellow*) is immobilized to the transducers surface. The sample is incubated separately with constant concentrations of antibody (*blue*) in the second step, followed by the injection of the incubated sample to the transducers surface. In step four, the bound antibody is detected

lowest. In the second run, the sequence is inverted, and again in the third run. Later measurements were done without order, but no differing results were obtained (data not shown).

For calibration in serum as matrix, human cystatin C-free serum was used in a 1:10 dilution with PBS. The serum concentration is kept constant in every sample, to avoid concentration dependent effects on the sensitive layer caused by serum constituent parts. Samples are spiked with defined cystatin C concentrations for calibration.

Data evaluation

The obtained binding curve involves a linear section, namely at the beginning of the sample injection.

The data are evaluated by applying a linear fit to this section. Plotting the slope of this fit versus the concentration of cystatin C on a semi logarithmic scale leads to a dataset that can be fitted by a four-parameter function (Eq. 1) of the form:

$$y = A_2 + \frac{(A_1 - A_2)}{1 + \left(\frac{x}{x_0}\right)^p} \tag{1}$$

Here A_1 is the lower asymptote and A_2 is the upper asymptote in the case of a binding-inhibition assay. The inflection point is given by the variable x_0, and the slope of the tangent in this point equates to the parameter p. This function describes a sigmoid curve progression which is an accepted approach to evaluate immunoassay data [19]. All signal slopes are normalized to the mean value of the blank measurement (antibody without inhibition). Additionally, the 95% confidence interval is plotted.

As defined in IUPAC guidelines [20], the limit of detection and limit of quantification can only be calculated if the sample concentrations in the calibration curve are equidistant. As this is not the case here, an alternative method is used for quantitative data evaluation.

The range in which the calibration curve can be used to quantify the analyte can be given by the minimum detectable concentration (MDC) and the reliable detection limit (RDL) [21]. These values are calculated by applying a tangent to the lower confidence limit at zero concentration (blank value). The intersection with the calibration curve itself marks the MDC whereas the intersection with the upper confidence limit marks the RDL. The working range is determined by applying the tangent to the upper confidence limit at zero signal. The intersection with the lower confidence limit together with the RDL comprises the working range.

Determination of recovery rates

Recovery rates are determined by threefold measurement of each concentration. Each value is normalized relative to the blank signal of the sensor chip. The mean value of the signal slopes is set as y in the four-parameter logistic function used for calibration. After solving the logistic function for x (Eq. 2), the aberrance of the calculated concentration and the real concentration is given as recovery rate.

$$x = \sqrt[p]{\frac{A_1 - A_2}{y - A_2} - 1} \cdot x_0 \tag{2}$$

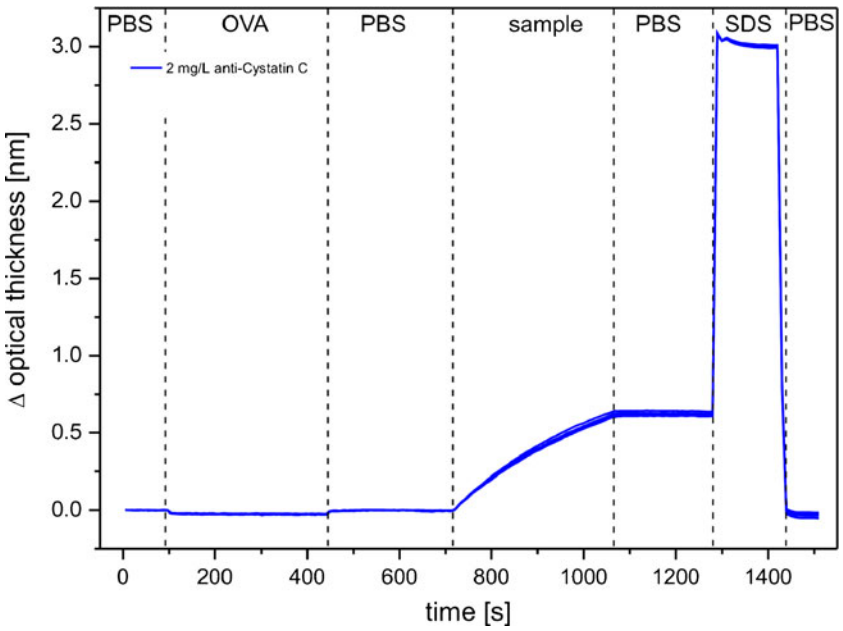

Fig. 2 Fourfold measurement with 2 mg/L cystatin C antibody of type (A). A constant concentration of 2 mg/L anti-cystatin C is detected four times. Unspecific binding is blocked with an ovalbumin (OVA) solution of 1 mg/mL in PBS. The surface is regenerated by a SDS solution of 0.5%/pH 2

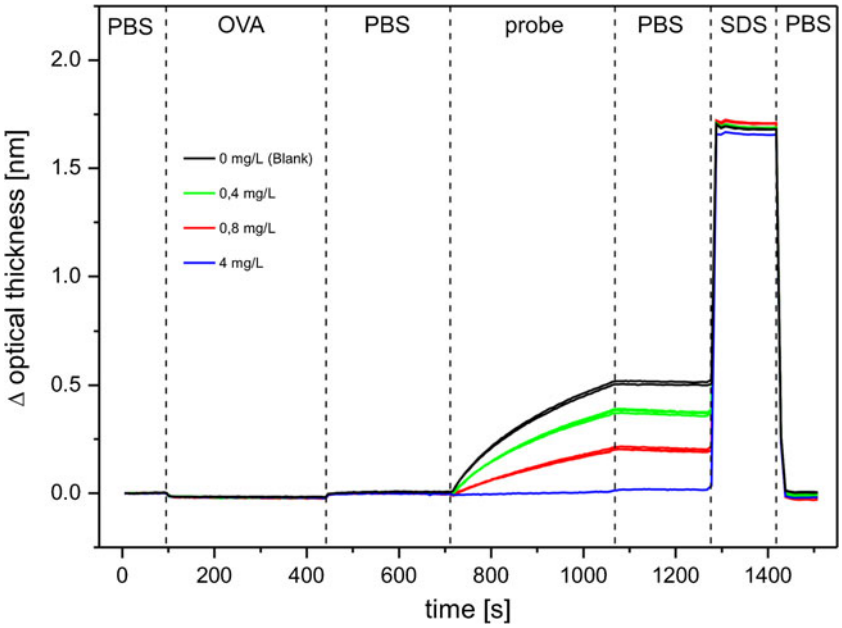

Fig. 3 Binding curves with 4 mg/L of antibody (A), inhibited with 0.4/0.8/4 mg/L cystatin C. A constant concentration of 4 mg/L antibody (A) is incubated with 0.4/0.8/4 mg/L cystatin C. Unspecific binding is blocked with an ovalbumin (OVA) solution of 1 mg/mL in PBS. The surface is regenerated by a SDS solution of 0.5%/pH 2

Results and discussion

Compared with other label-free techniques such as SPR or integrated optical devices, the main advantage of RIfS is the low-temperature dependence of the obtained binding signals.

Detecting refractive index changes in the sensitive layer with SPR requires strict temperature control and referencing. This involves a relatively complex instrumentation setup [22].

Using RIfS for detecting biomolecular interactions at a sensitive layer, temperature control is not required. Volume increases caused by increasing temperature in the sensitive layer are nearly compensated by a refractive index decrease with rising temperature. In addition, transparent transducer substrates, such as glass or polymers, are used and no expensive gold surface is needed. This is why the experimental setup can be kept comparatively simple and therefore cost-effective.

For performing a binding-inhibition assay, it is necessary to immobilize the analyte to the transducers surface. This step can be critical, especially in the case of proteins, because the epitope, which is detected in the later step by the antibody, has to remain unaffected by the coupling conditions. To optimize the immobilization process, first, measurements were done in PBS buffer. Figure 2 shows the binding curve of 2 mg/L monoclonal antibody of type (A) to an aminodextran surface with covalently immobilized cystatin C.

The binding curves show high inner chip reproducibility. All four measurements could be done on the same transducer by regenerating the sensitive layer with SDS.

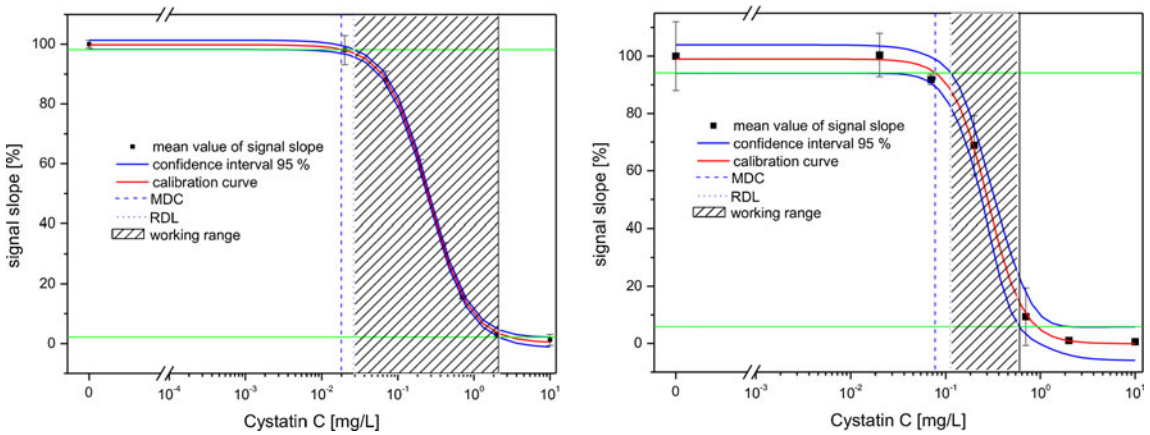

Fig. 4 Calibration curves in PBS as matrix. *Left side* Antibody (A). *Right side* Antibody (B). *Left side* A constant concentration of 1.5 mg/L cystatin C antibody (A) is inhibited by eight different concentrations of cystatin C ranging from 0 to 10 mg/L. Every concentration is determined threefold. *Right side* A constant concentration of 1.5 mg/L cystatin C antibody (A) is inhibited by seven different concentrations of cystatin C ranging from 0 to 10 mg/L. Every concentration is determined threefold. PBS is used as matrix for both calibrations

Table 1 MDC and RDL values with the resulting working range for antibody (A) and (B) in PBS

Antibody type	MDC [mg/L]	RDL [mg/L]	Working range [mg/L]
(A)	0.018	0.026	0.026–2.113
(B)	0.077	0.112	0.112–0.604

With label-free detection methods such as RIfS, unspecific binding to the sensitive layer can cause problems. With binding curves as shown in Fig. 2, it is not proven that the antibody binds specifically with its paratope to the epitope on the immobilized cystatin C. Changes in the optical thickness would also occur in a comparable way if the antibody is adsorbed with its Fab- or Fc-fragment. By inhibiting the antibody with the antigen in an incubation step, its binding sites should be (partially or fully) occupied, which impedes (or lowers) binding to the surface during the detection step. This can be seen as a proof for low cross-sensitivity.

In Fig. 3, measurements are shown where the antibody (A) is inhibited with defined concentrations of cystatin C.

Inhibiting the antibody leads to graded signals, depending on the antigen concentration in the sample. Incubating the antibody for 20 min in a 10:1 molar ratio with cystatin C leads to completely saturated binding sites of the antibody and no binding events to the surface can be detected.

Based on these results, we calibrated a single chip using a binding-inhibition assay as described with PBS buffer as matrix. Figure 4 shows the calibration curve for the antibody of type (A) and the same for the antibody of type (B), to compare the behavior of different monoclonal antibody strains.

MDC and RDL values are given in the following Table 1.

The result is a calibration curve for (A) covering two magnitudes of cystatin C concentration with its dynamic region. The antibody (B) results in a narrower dynamic range and seems to bind less specific, as the standard deviations are wider. For the antibody (A), the working range of the calibration curve fits well to the demanded clinical limits between 0.53 and 1.02 mg/L.

Table 2 MDC and RDL values with the resulting working range for antibody (A) and (B) in serum

Antibody type	MDC [mg/L]	RDL [mg/L]	Working range [mg/L]	Working range [mg/L]×10
(A)	0.061	0.096	0.096–0.660	0.96–6.60
(B)	0.052	0.067	0.067–0.257	0.67–2.57

As previous investigations have shown no difference of cystatin C concentration in plasma, serum, or full blood, serum concentration also refers to the plasma or full blood level and is normally used as matrix [6]. Thus, for quantification with real clinical samples, we established the assay in serum. This can result in further problems in immunoassays, as serum components can interact either with the surface and the immobilized antigen or with the antibody, influencing the antigen–antibody interaction. To prevent serum components from binding to the sensitive layer, FCS is used to block unspecific binding. Based on the calibrations in buffer for the two antibody types, further measurements were done with serum as matrix, and the two antibodies were again calibrated. Figure 5 shows the obtained functions.

In the case of a renal failure, the serum level of cystatin C will rise. Therefore, it is important to be able to quantify at and above the upper limit of cystatin C concentration in healthy individuals. In particular, the antibody (B) can fulfill these requirements. The MDC and RDL values are given with the resulting working range in Table 2. As serum

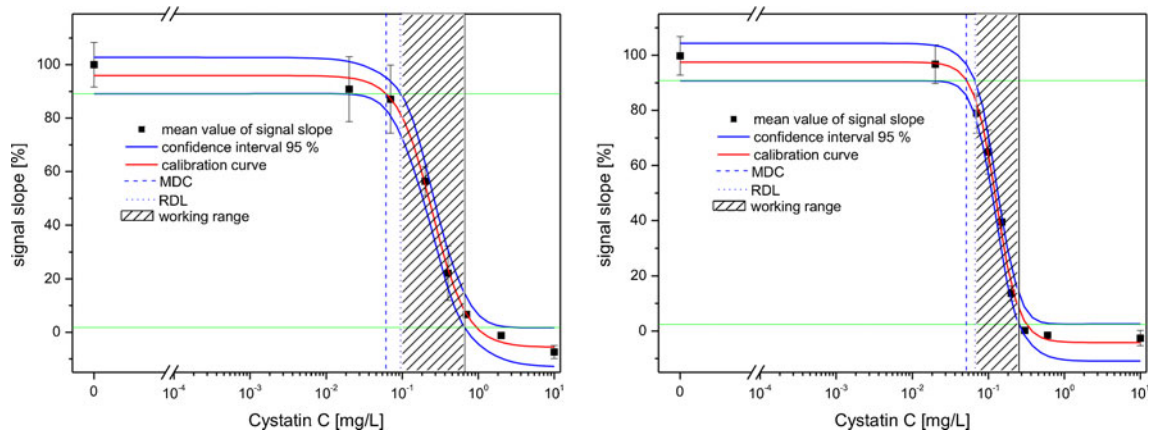

Fig. 5 Calibration curves in serum 1:10 as matrix. *Left side* Antibody (A). *Right side* Antibody (B). *Left side* A constant concentration of 1.5 mg/L cystatin C antibody (A) is inhibited by eight different concentrations of cystatin C ranging from 0 to 10 mg/L. Every concentration is determined threefold. *Right side* A constant concentration of 1.5 mg/L cystatin C antibody (A) is inhibited by nine different concentrations of cystatin C ranging from 0 to 10 mg/L. Every concentration is determined threefold. Human cystatin C-free serum is used as matrix for both calibrations

Table 3 Recovery rates determined on two additional sensor chips, based on calibration for (B) in serum

	Signal slope [%]	Detect. Conc. [mg/L]	Real conc. [mg/L]	Recovery rate [%]
Chip 1	70.58	0.090	0.08	112.9
	63.63	0.101	0.10	100.9
Chip 2	70.57	0.090	0.08	112.9
	46.92	0.127	0.15	84.8
	0.81	0.348	0.3	116.1

was used in a 1:10 dilution with PBS, the working range has to be multiplied by a factor 10 to compare it with the relevant clinical limits.

In contrast to our expectations based on the results in buffer, the antibody (B) shows better results in serum as antibody (A). The reason for that cannot be enlightened completely within the scope of this work. In fact, antibodies can behave particularly different in their "native surroundings" serum, plasma, or blood. Antibody (B) enables to quantify the protein in human serum within the clinical ranges of 0.53–1.02 mg/L.

To support the promising results with antibody (B), we determined recovery rates for several concentrations. To demonstrate the high chip to chip reproducibility of the sensors, these measurements were done on two additional transducers. The results are shown in Table 3.

These results demonstrate the possibility to calibrate one sensor chip and to do the measurements on a second or third chip using the same calibration. This enables the user to choose, if he would like to do several measurements on one chip or to use the sensor chips as disposables which might be important in terms of hygiene and cross contamination.

Conclusion

The aim was to establish a label-free assay based on RIfS, to quantify cystatin C in the required clinical range fast, simple, and cost-effective. We chose the binding-inhibition assay as the assay format. Therefore, the antigen has to be attached to the transducers surface. We were able to show that the protein could be immobilized with the epitope in its native state. It could be demonstrated that the attached protein is stable and that the antigen–antibody complex can be disengaged, so several measurements can be made on a single chip. By comparing two different commercially available, monoclonal antibodies, we optimized the results in terms of specificity of antigen–antibody interaction and dynamic region of the obtained calibration curve. The behavior of the two compared antibodies was particularly different in buffer and in serum as matrix.

Sensor chips with immobilized cystatin C were first calibrated using buffer as matrix. Comparing the two monoclonal antibody types, (A) shows better results in buffer as the dynamic region covers full two magnitudes of cystatin C concentration. Compared to that, the antibody type (B) shows more unspecific binding and a reduced dynamic range.

The results in serum are contrary. Here, the antibody type (B) hits the required detection limit and the signals are more reproducible. With this antibody, it was possible to calibrate a single chip. The obtained calibration can be used to quantify cystatin C within the relevant clinical range on any chip that was processed the same way as the calibration chip. The quantification can be done within several minutes for one measurement, which can be seen as fast enough for emergency diagnostics. As the RIfS setup is compact and simple to handle, it already provides many possibilities for point-of-care applications. Further work will be done to transfer the established assay to a portable handheld device for POCT.

Acknowledgments This work was partially funded by the Bundesministerium für Wirtschaft und Technologie (BMWI) and the Allianz Industrie und Forschung (AIF) within the project "ACUTLAB," IGF-Nr.: 16696 N1.

References

1. Tjan HL, Tobias GJ, Levin R, Hopper J Jr (1963) Creatinine clearance in clinical medicine. Calif Med 98:121–128
2. Bicik Z, Bahcebasi T, Kulaksızoglu S, Yavuz O (2005) The efficacy of cystatin C assay in the prediction of glomerular filtration rate. Is it a more reliable marker for renal failure? Clin Chem Lab Med 43(8):855–861. doi:10.1515/cclm.2005.144
3. Shemesh O, Golbetz H, Kriss JP, Myers BD (1985) Limitations of creatinine as a filtration marker in glomerulopathic patients. Kidney Int 28(5):830–838
4. Kazama JJ, Kutsuwada K, Ataka K, Maruyama H, Gejyo F (2002) Serum cystatin C reliably detects renal dysfunction in patients with various renal diseases. Nephron 91(1):13–20. doi:10.1159/000057599
5. Lock EA (2010) Sensitive and early markers of renal injury: where are we and what is the way forward? Toxicol Sci 116(1):1–4. doi:10.1093/toxsci/kfq128
6. Grubb AO (2001) Cystatin C-properties and use as diagnostic marker. Adv Clin Chem 35:63–99
7. Finney H, Newman DJ, Price CP (2000) Adult reference ranges for serum cystatin C, creatinine and predicted creatinine clearance. Ann Clin Biochem 37(1):49–59
8. Käppel N (2007) Immunoassay-Optimierung für verschiedene probenmatrices. Dissertation, Eberhard Karls Universität, Tübingen
9. Albrecht C, Kaeppel N, Gauglitz G (2008) Two immunoassay formats for fully automated CRP detection in human serum. Anal Bioanal Chem 391(5):1845–1852. doi:10.1007/s00216-008-2093-x

10. Fechner P, Proell F, Carlquist M, Proll G (2009) An advanced biosensor for the prediction of estrogenic effects of endocrine-disrupting chemicals on the estrogen receptor alpha. Anal Bioanal Chem 393(6–7):1579–1585. doi:10.1007/s00216-008-2480-3
11. Cheskis B, Freedman LP (1996) Modulation of nuclear receptor interactions by ligands: kinetic analysis using surface plasmon resonance. Biochemistry 35(10):3309–3318. doi:10.1021/bi952283r
12. Ingenhoff J, Drapp B, Gauglitz G (1993) Biosensors using integrated optical devices. Fresenius J Anal Chem 346(6–9):580–583
13. Gauglitz G (2010) Direct optical detection in bioanalysis: an update. Anal Bioanal Chem 398(6):2363–2372. doi:10.1007/s00216-010-3904-4
14. Hänel G (2002) Comparison of reflectometric interference spectroscopy with other instruments for label-free optical detection. Anal Bioanal Chem 372(1):91–100. doi:10.1007/s00216-001-1197-3
15. Proell F, Moehrle B, Kumpf M, Gauglitz G (2005) Label-free characterization of oligonucleotide hybridization using reflectometric interference spectroscopy. Anal Bioanal Chem 382 (8):1889–1894. doi:10.1007/s00216-005-3301-6
16. Gauglitz G, Luppa PB (2009) Point-of-care laboratory testing. Chem Unserer Zeit 43(5):308–318
17. Moehrle BP, Kumpf M, Gauglitz G (2005) Determination of affinity constants of locked nucleic acid (LNA) and DNA duplex formation using label free sensor technology. Analyst (Cambridge, United Kingdom) 130(12):1634–1638. doi:10.1039/b507728a
18. Brecht A, Gauglitz G, Nahm W (1992) Interferometric measurements used in chemical and biochemical sensors. Analusis 20 (3):135–140
19. Dudley RA, Edwards P, Ekins RP, Finney DJ, McKenzie IG, Raab GM, Rodbard D, Rodgers RP (1985) Guidelines for immunoassay data processing. Clin Chem 31(8):1264–1271
20. Inczedy J (1998) Compendium of analytical nomenclature. 3rd edn. Blackwell
21. O'Connell MA, Belanger BA, Haaland PD (1993) Calibration and assay development using the four-parameter logistic model. Chemom Intell Lab Syst 20(2):97–114
22. Joensson U, Faegerstam L, Ivarsson B, Johnsson B, Karlsson R, Lundh K, Loefaas S, Persson B, Roos H et al (1991) Real-time biospecific interaction analysis using surface plasmon resonance and a sensor chip technology. Biotechniques 11(5):620–622, 624–627